

## **Dual-Functional Two-Dimensional Covalent Organic Frameworks for Water Sensing and Harvesting**

Shan Jiang,<sup>a</sup> Lingchen Meng,<sup>a</sup> Wenyue Ma,<sup>a</sup> Guocui Pan,<sup>a</sup> Wei Zhang,<sup>c</sup> Yongcun Zou,<sup>b</sup> Leijing Liu<sup>\*a</sup>, Bin Xu,<sup>a</sup> Wenjing Tian<sup>\*a</sup>

<sup>a</sup> State Key Laboratory of Supramolecular Structure and Materials, College of Chemistry, Jilin University, Changchun 130012, China.

<sup>b</sup> State Key Laboratory of Inorganic Synthesis and Preparative Chemistry, College of Chemistry, Jilin University, Changchun 130012, China.

<sup>c</sup> Electron Microscopy Center, Jilin University, Changchun 130012, China

### **Contents**

1. Experimental Section
2. Supplementary Figures and Tables
3. Reference

## 1. Instruments and methods

The solid-state  $^{13}\text{C}$  cross-polarization/magic-angle spinning (CP/MAS) NMR spectra were obtained using a Bruker AVANCE III 400 WB spectrometer. Powder X-ray diffraction data were recorded by a Rigaku 2550 diffractometer with  $\text{Cu}\cdot\text{K}\alpha$  radiation ( $\lambda = 1.5418 \text{ \AA}$ ) at 298K (scan range: 2-40°). Fourier transform infrared (FTIR) spectra were recorded on a Vertex 80V spectrometer (Germany). TGA was carried out using a TA Q500 thermogravimeter from room temperature to 800 °C under an air atmosphere at the heating rate of 10 °C  $\text{min}^{-1}$  under a nitrogen atmosphere. Elemental analyses were performed using a Vario Micro (Elementar) spectrometer. Scanning electron microscope (SEM) images were recorded on scanning electron microscopy, JEOL JSM 6700F (Japan). Transmission electron microscope (TEM) images were recorded on a JEM-2100F instrument with an accelerating voltage of 200 kV. The sample was prepared by placing a drop of the stock solution on a 300-mesh, carbon coated copper grid and air-dried before measurement. UV-Vis spectra were recorded with a Shimadzu UV-2550 spectrophotometer (Japan). Fluorescence spectroscopy was taken with a Shimadzu RF-5301 PC spectrometer. The gas adsorption–desorption measurements at different temperatures were carried out using the Micromeritics ASAP 2020 instrument. The samples were degassed at 120 °C under vacuum for 10 h. Water adsorption was carried out by using IGAcorp dynamic moisture sorption analyzer (DVS) of Hiden company.

## 2. Supplementary Figures and Tables

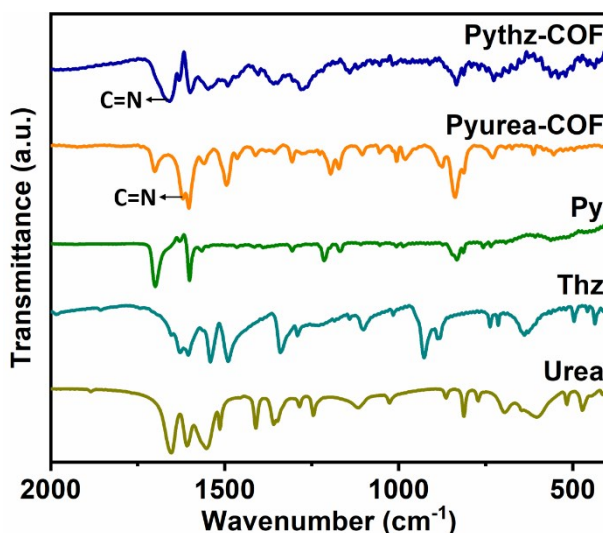


**Figure S1.** FTIR spectra of Py, Thz, Urea, Pythz-COF and Pyurea-COF.

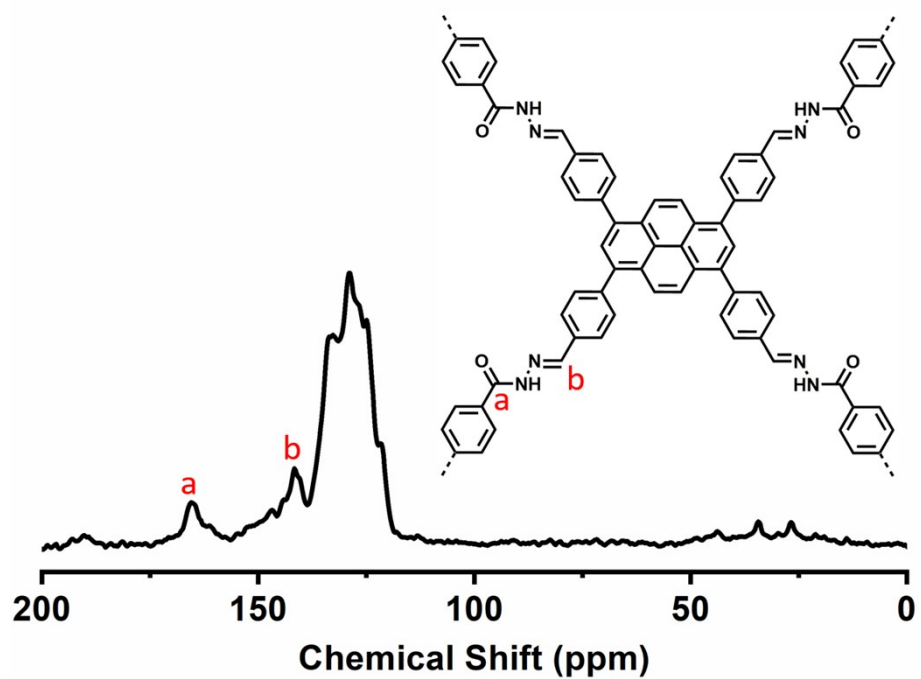


**Figure S2.** Solid-state  $^{13}\text{C}$  CP/MAS NMR spectrum of Pythz-COF.

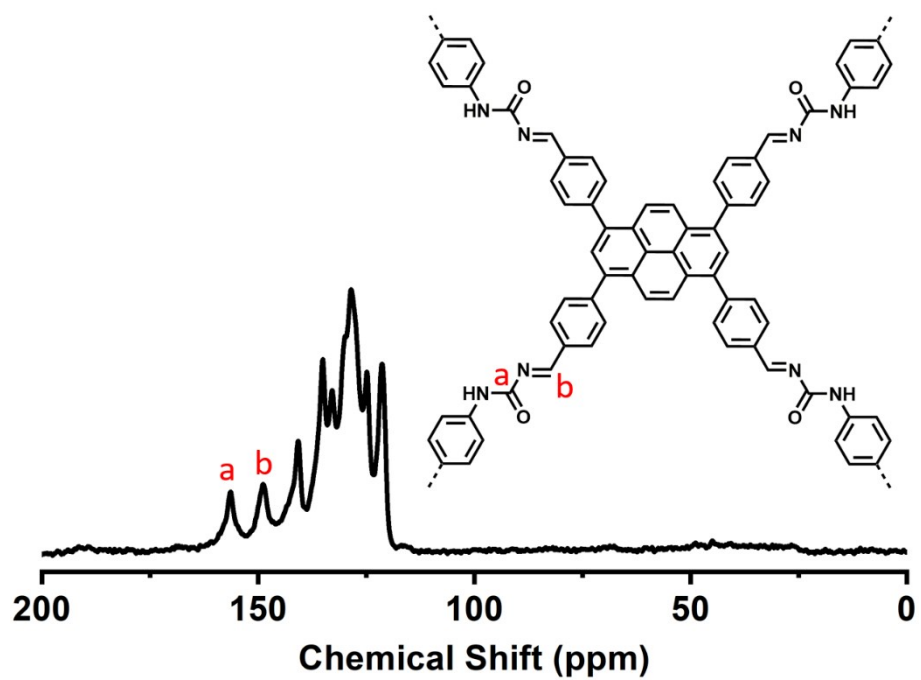


**Figure S3.** Solid-state  $^{13}\text{C}$  CP/MAS NMR spectrum of Pyurea-COF.

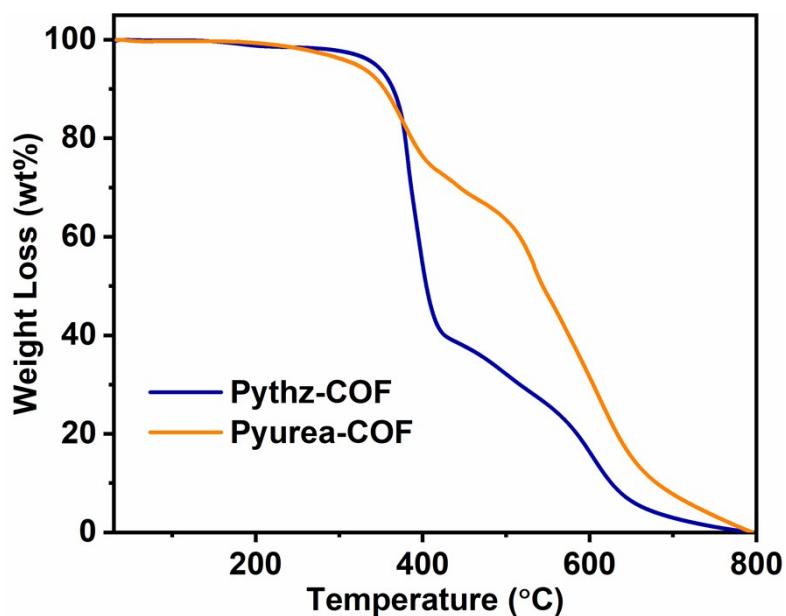


**Figure S4.** TGA profiles of Pythz-COF and Pyurea-COF.

**Table S1.** Atomic coordinates for the unit cell of Pythz-COF with AA-stacking.

Sample Name: Pythz-COF				
Space Group: CMM2 (orthorhombic)				
$a = 38.4962, b = 42.6997, c = 3.7970; \alpha = \beta = \gamma = 90^\circ$				
$R_p = 5.63\%, R_{wp} = 7.78\%$				
Atom	Type	x/a	y/b	z/c
C1	C	0.51803	0.44357	0.06609
C2	C	0.53696	0.47117	0.0068
C3	C	0.42626	0.47126	-0.02667
C4	C	0.40379	0.44269	-0.04239
C5	C	0.4137	0.41572	-0.22985
C6	C	0.39225	0.38935	-0.23998
C7	C	0.35969	0.38973	-0.07536
C8	C	0.34882	0.41705	0.09824
C9	C	0.37064	0.44315	0.11534
C10	C	0.33748	0.36162	-0.09007
C11	C	0.72698	0.72392	0.07244
C12	C	0.71423	0.7548	0.06881
C13	C	0.73676	0.78044	0.06496
C14	C	0.70193	0.69715	0.07694
N15	N	0.69038	0.64041	0.10206
O16	O	0.17094	0.20292	0.05824
N17	N	0.21277	0.16654	0.1129
H18	H	0.53058	0.42154	0.11938
H19	H	0.43777	0.41504	-0.37476
H20	H	0.40085	0.36879	-0.38262

H21	H	0.32368	0.41816	0.22539
H22	H	0.36175	0.46359	0.25822
H23	H	0.3447	0.34289	-0.26736
H24	H	0.68655	0.75932	0.06722
H25	H	0.72516	0.8034	0.0529
H26	H	0.23817	0.1618	0.18969
C27	C	0.48148	0.5	0.00127
C28	C	0.40923	0.5	-0.04677

**Table S2.** Atomic coordinates for the unit cell of Pyurea-COF with AA-stacking.

Sample Name: Pyurea-COF				
Space Group: P-1 (triclinic)				
a = b = 24.1230, c = 4.6602; $\alpha = 87.8411^\circ$ , $\beta = 92.7384^\circ$ , $\gamma = 97.5733^\circ$				
$R_p = 6.27\%$ , $R_{wp} = 8.16\%$				
Atom	Type	x/a	y/b	z/c
C1	C	-0.18069	-0.34077	1.38504
N2	N	-0.07696	-0.42545	1.59415
C3	C	-0.03869	-0.46199	1.54398
C4	C	-0.03969	0.48784	1.70372
C5	C	0.002	-0.45055	1.33972
C6	C	0.66212	0.21187	1.47261
N7	N	0.59008	0.0798	1.34127
C8	C	0.54556	0.03947	1.4201
C9	C	0.55125	0.00104	1.6469
C10	C	0.4936	0.03765	1.27412
C11	C	0.37521	-0.2544	1.55651
C12	C	0.42172	-0.25027	1.75355
C13	C	0.3662	-0.30139	1.3828
C14	C	0.45775	-0.28989	1.77541
C15	C	0.4018	-0.34147	1.39782
C16	C	0.44967	-0.33743	1.59591
C17	C	0.48887	-0.37628	1.59943
C18	C	0.47161	-0.43524	1.59137
C19	C	0.54628	-0.35708	1.59058
C20	C	0.50931	-0.47183	1.52012
C21	C	0.41623	-0.458	1.65131
C22	C	0.58597	-0.39318	1.54449
C23	C	0.56591	-0.45073	1.48768
C24	C	0.39792	-0.51328	1.61097
C25	C	0.64334	-0.37272	1.54032
C26	C	0.68368	-0.3983	1.71918
C27	C	0.66541	-0.33108	1.3313
C28	C	0.73984	-0.38749	1.67148

C29	C	0.72195	-0.32128	1.28924
C30	C	0.76064	-0.3498	1.45181
O31	O	-0.09595	-0.39191	1.13678
O32	O	0.60299	0.12223	1.77609
N33	N	-0.14643	-0.37065	1.5219
C34	C	-0.1046	-0.39513	1.3923
N35	N	0.64469	0.16374	1.36449
C36	C	0.61238	0.12145	1.52178
H37	H	-0.16452	-0.30807	1.21553
H38	H	-0.0879	-0.41845	1.81742
H39	H	-0.07198	0.47673	1.87442
H40	H	0.00471	-0.40994	1.20482
H41	H	0.70531	0.21949	1.58531
H42	H	0.60827	0.07858	1.12761
H43	H	0.59321	0.00112	1.77038
H44	H	0.48746	0.06828	1.08656
H45	H	0.43029	-0.21316	1.90089
H46	H	0.32855	-0.30696	1.2243
H47	H	0.49474	-0.28522	1.93817
H48	H	0.39368	-0.37879	1.25172
H49	H	0.56197	-0.31092	1.62128
H50	H	0.38624	-0.43014	1.7344
H51	H	0.35291	-0.53093	1.65704
H52	H	0.66923	-0.42813	1.90433
H53	H	0.63593	-0.30589	1.19889
H54	H	0.77105	-0.40925	1.8115
H55	H	0.73878	-0.2892	1.11833

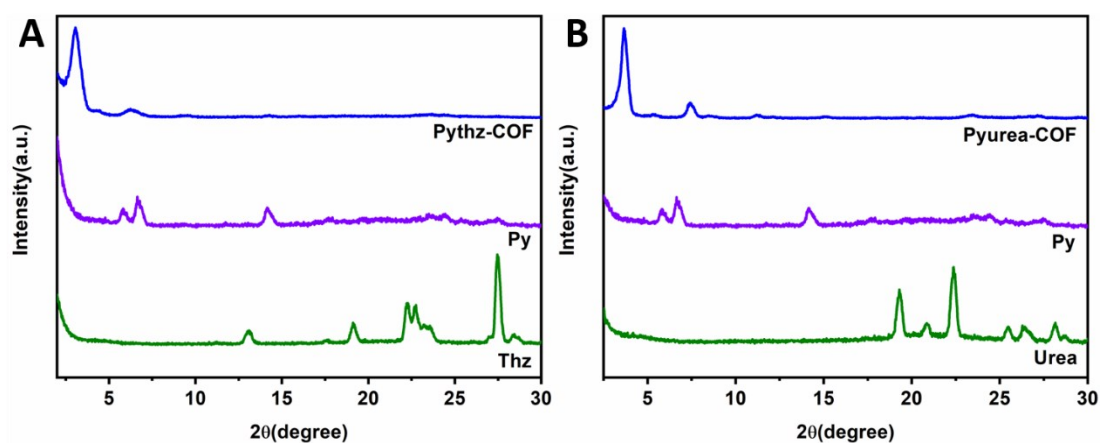


**Figure S5.** A) PXRD patterns of Pythz-COF, Py and Thz. B) PXRD patterns of Pyurea-COF, Py and Urea.

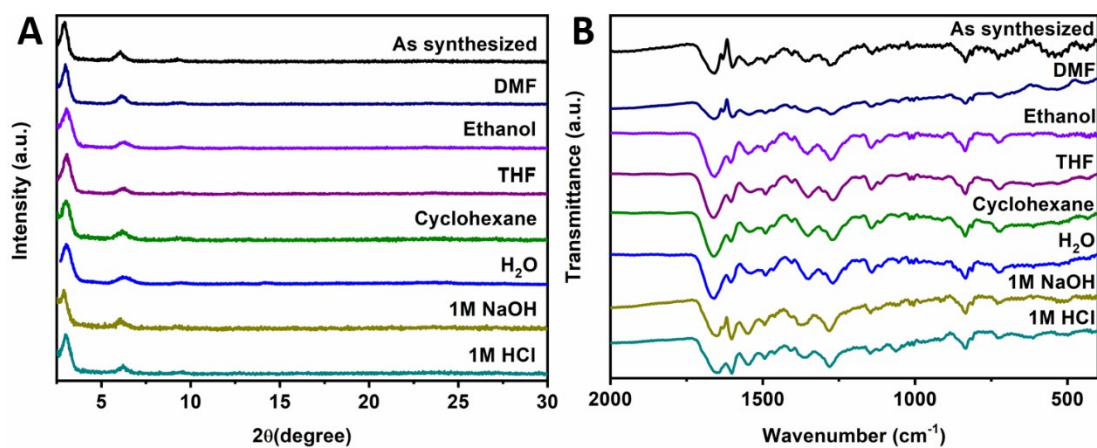


**Figure S6.** A) XRD patterns and B) FT-IR spectra of Pythz-COF upon treatment in different solvents.

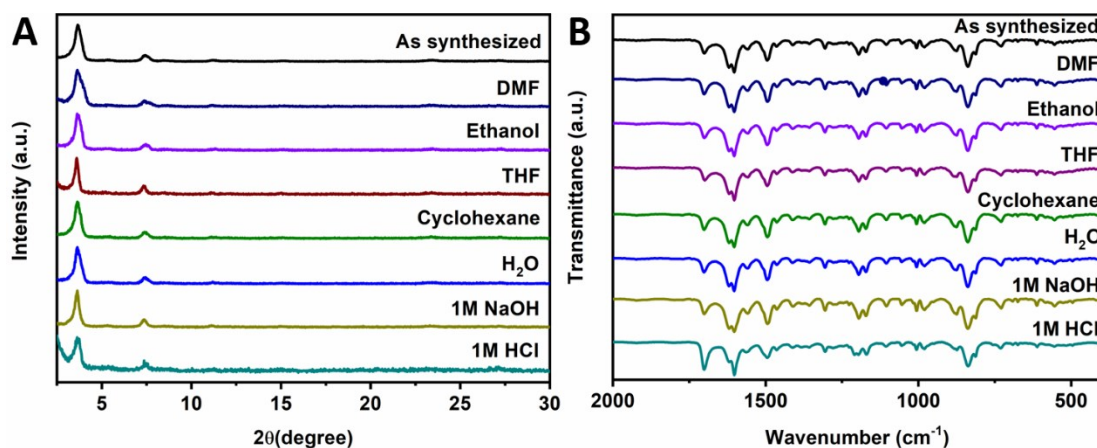


**Figure S7.** A) XRD patterns and B) FT-IR spectra of Pyurea-COF upon treatment in different solvents.

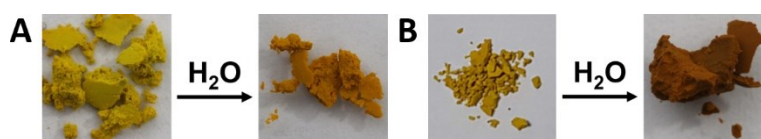


**Figure S8.** A) Photographs of the dry and wet Pythz-COF. B) Photographs of the dry and wet Pyurea-COF.

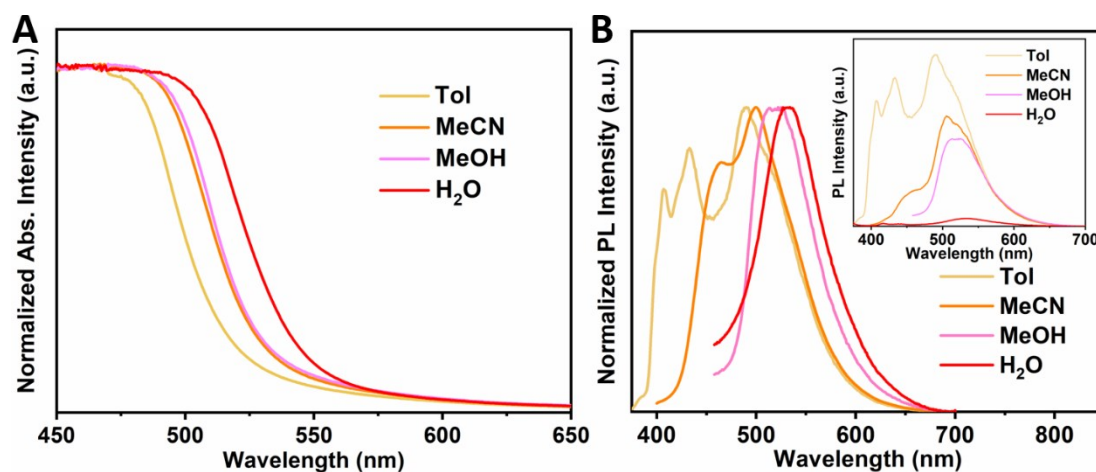


**Figure S9.** A) Solid-state UV-Vis absorption spectra of Pythz-COF soaked by various polarity solvents. B) PL spectra of Pythz-COF in various polarity solvents (0.1mg/ml).

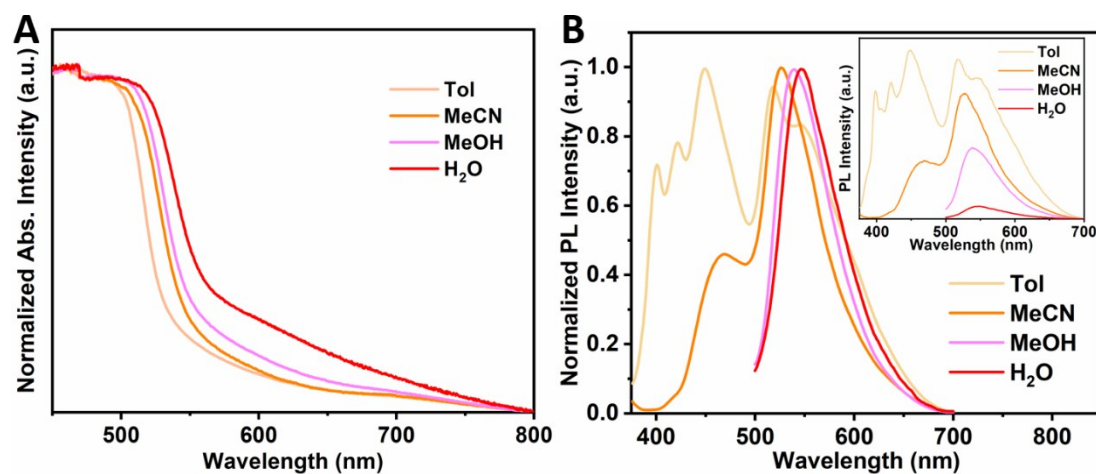


**Figure S10.** A) Solid-state UV-Vis absorption spectra of Pyurea-COF soaked by various polarity solvents. B) PL spectra of Pyurea-COF in various polarity solvents (0.1mg/ml).



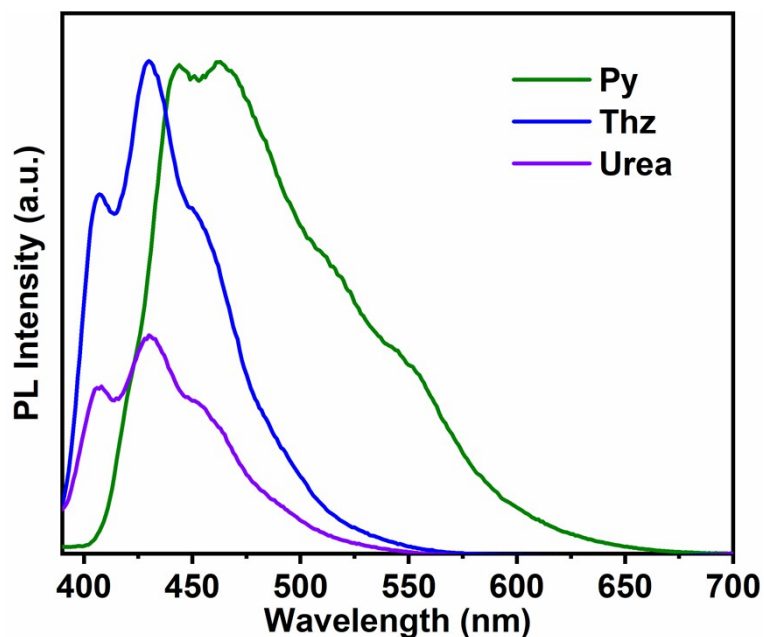


**Figure S11.** The PL spectra of the monomers (Py, Thz and Urea) in acetonitrile ( $10^{-5}$  mol/L).

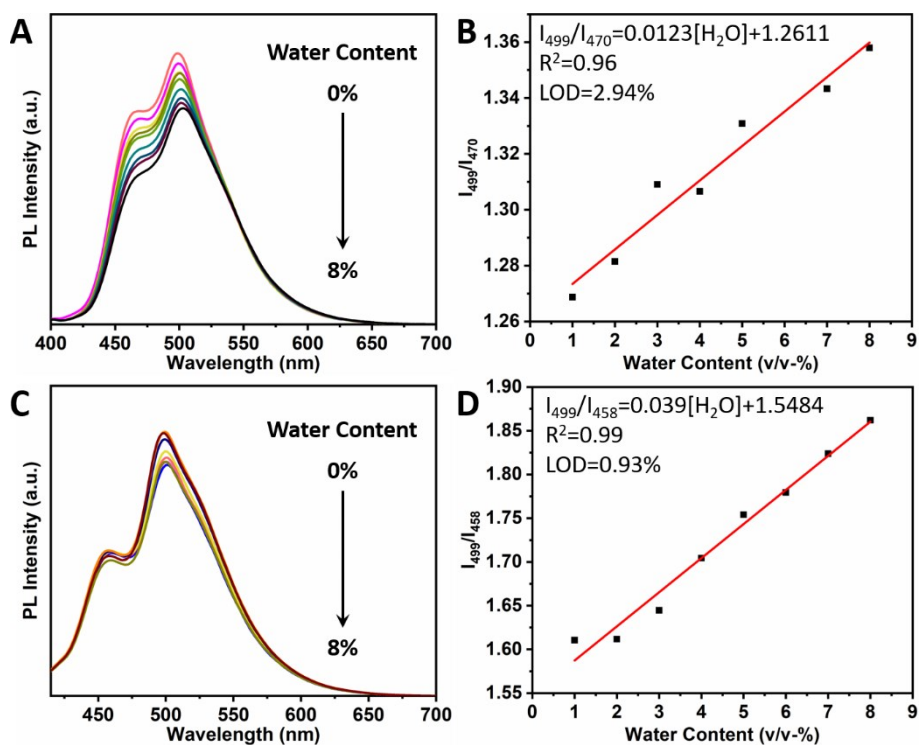


**Figure S12.** A) PL spectra of Pythz-COF in *N,N*-Dimethylformamide with trace content of water. B) The linear correlation between the fluorescence of Pythz-COF and different water contents in *N,N*-Dimethylformamide. C) PL spectra of Pythz-COF in tetrahydrofuran with trace content of water. D) The linear correlation between the fluorescence of Pythz-COF and different water contents in tetrahydrofuran.

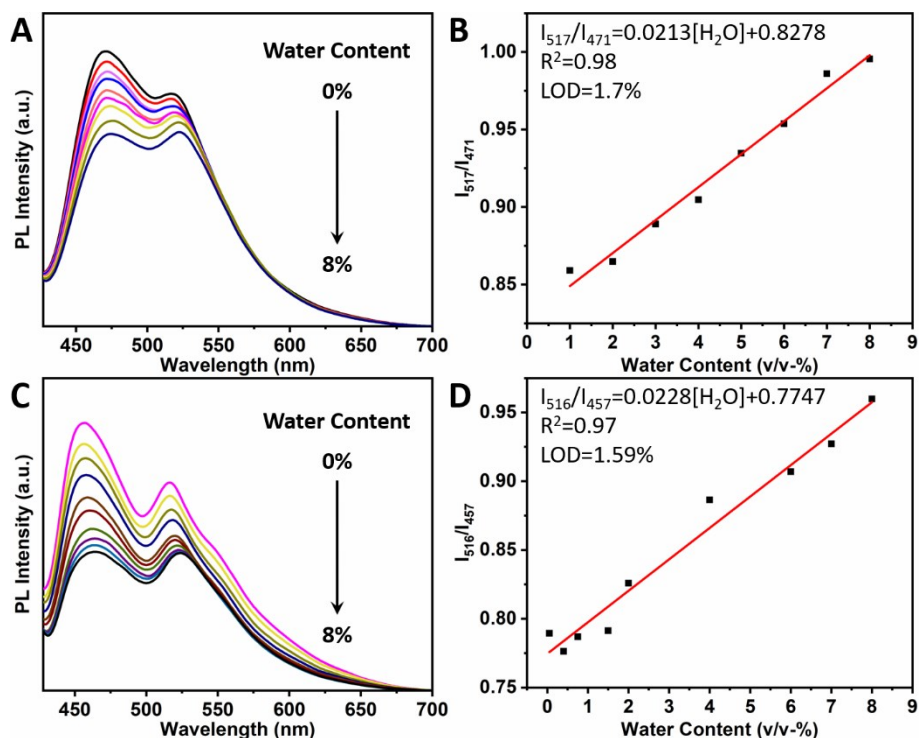


**Figure S13.** A) PL spectra of Pyurea-COF in N,N-Dimethylformamide with trace content of water. B) The linear correlation between the fluorescence of Pyurea-COF and different water contents in N,N-Dimethylformamide. C) PL spectra of Pyurea-COF in tetrahydrofuran with trace content of water. D) The linear correlation between the fluorescence of Pyurea-COF and different water contents in tetrahydrofuran.

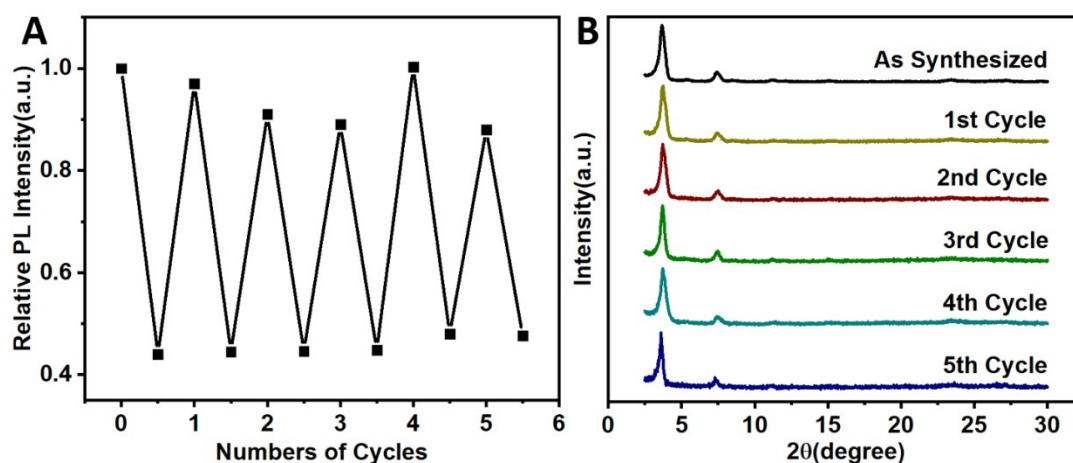


**Figure S14.** A) Reversible switching of relative PL intensity of Pyurea-COF with or without being added water (7%), em: 527nm. B) PXR patterns of Pyurea-COF after different cycles of trace water sensing (7%).

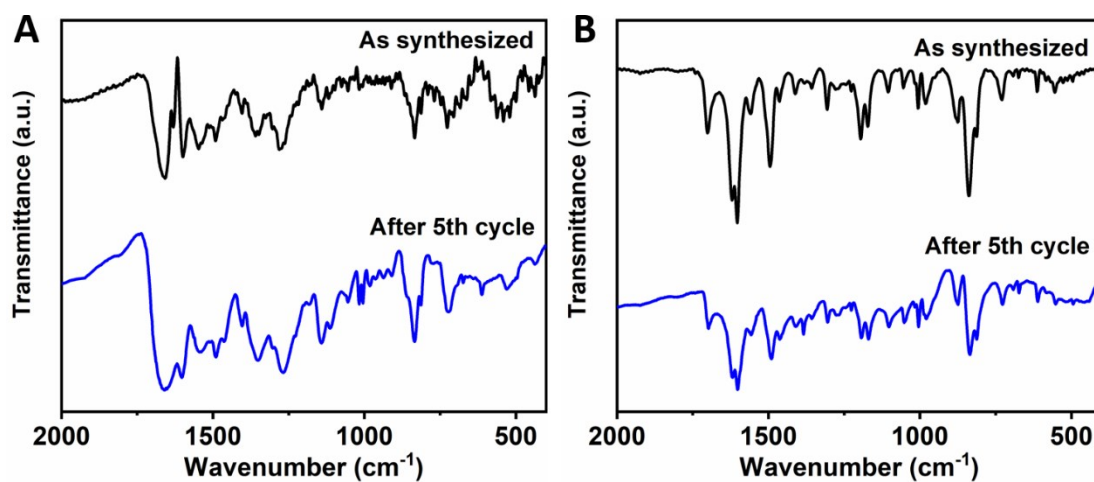


**Figure S15.** FTIR spectra of A) Pythz-COF and B) Pyurea-COF before and after 5 cycles of trace water sensing.

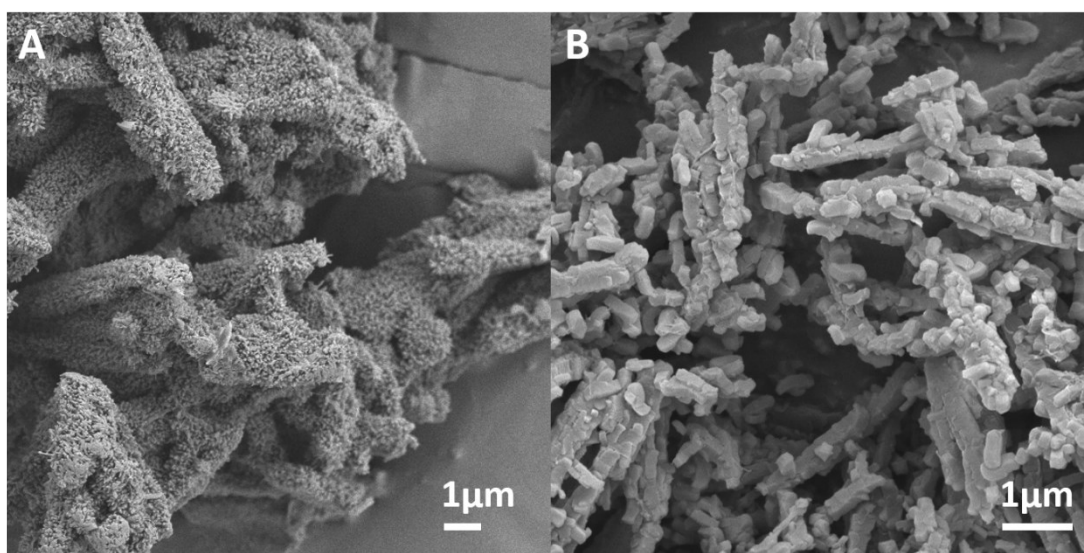


**Figure S16.** SEM images of A) Pythz-COF and B) Pyurea-COF after 5 cycles of trace water sensing.

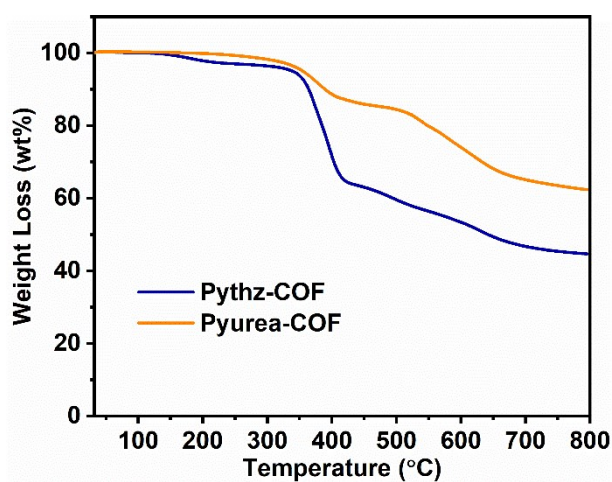


**Figure S17.** TGA profiles of Pythz-COF and Pyurea-COF after 5 cycles of trace water sensing.

**Table S3.** Comparison of the sensing performance of various materials toward water.

Materials	Type	Solvents	LOD	Ref.
Pythz-COF	COF	acetonitrile	0.09 (v/v-%)	This work
Pyurea-COF			0.02 (v/v-%)	
COFs	COF	methanol	0.042 (v/v-%)	1
TzDa	COF	EtAC	0.006 (wt-%)	2
COF-4-OH	COF	ethanol	0.03 (v/v-%)	3
TAPT-BMTA-COF	COF	acetonitrile	0.12 (v/v-%)	4
Tb <sub>97.11</sub> Eu <sub>2.89</sub> -L1	MOF	acetonitrile	0.04 (v/v-%)	5
AEMOF-1'	MOF	THF	0.05 (v/v-%)	6
PPQ-CDs	carbon dots	DMSO	0.023 (v/v-%)	7
RCDs	carbon dots	acetone	0.082% (v/v-%)	8
MOF@superparamagnetic	complex material	hexane	0.3 (wt-%)	9

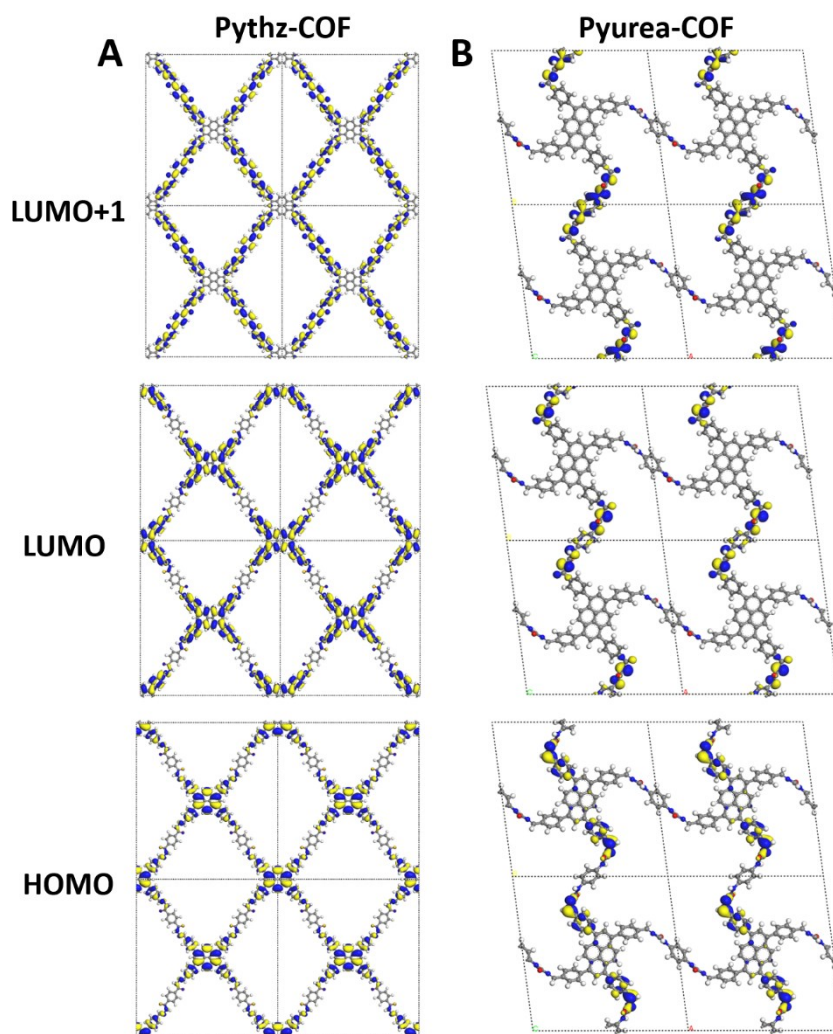




**Figure S18.** The frontier orbital contribution of the single-layer molecular structure of A) Pythz-COF and B) Pyurea-COF by DFT calculations.

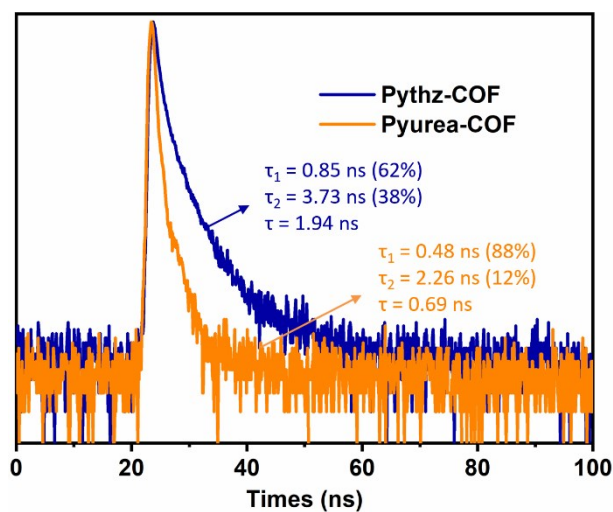


**Figure S19.** Fluorescence decay profiles of two COFs in solid state.

**Table S4.** Summary of textural properties of various materials along with their water uptake performance.

Materials	Type	BET surface area (m <sup>2</sup> /g)	Total pore volume (cm <sup>3</sup> /g)	H <sub>2</sub> O adsorption (mmol/g) <sup>b</sup>	H <sub>2</sub> O adsorption (wt%) <sup>b</sup>	Temperature (K)	Ref.
Pythz-COF	COF	1571	1.01	46.2	83.2	298	This work
Pyurea-COF		1016	0.53	35.8	64.5		
COF-432	COF	895	0.43	16.7	30	298	10
AB-COF	COF	1125	0.47	22.9	41	288	11
ATFG-COF		520	0.5	13.6	25		
DhaTab	COF	N/A <sup>a</sup>	N/A	31.7	57	298	12
TpPa-1	COF	1432	N/A	28.9	52	298	13
TpAzo		3038		22.7	41		
Trzn-COF	COF	408.5	N/A	2	4	298	14
2D ep-POP	POP	852	0.18	22.9	41.1	298	15
3D ep-POP		779	0.17	22.9	41.1		
KFUPM-1	POP	305	N/A	18.7	33.5	298	16
UiO-66	MOF	1160	0.52	20.5	37	298	17
UiO-66-NH <sub>2</sub>		1040	0.57	20.5	37		
UiO-67	MOF	2064	0.97	10	18	293	18
H <sub>2</sub> N-MIL-125		1220	0.55	20.5	37		

<sup>a</sup> N/A: Not available

<sup>b</sup> Condensation effects observed at higher humidity levels.

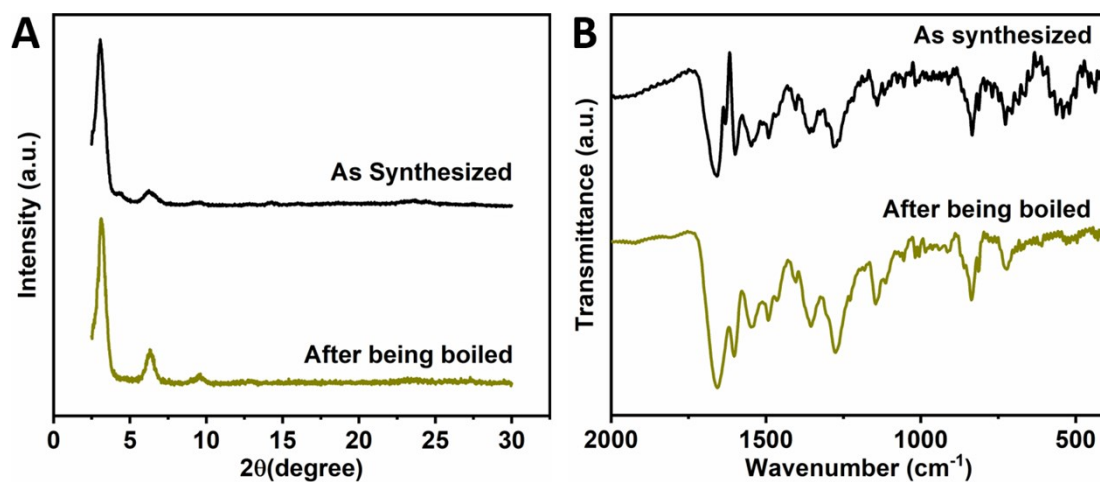


**Figure S20.** A) PXRD patterns and B) FTIR spectra of Pythz-COF before and after being boiled in hot water (80 °C) for 8 hours.

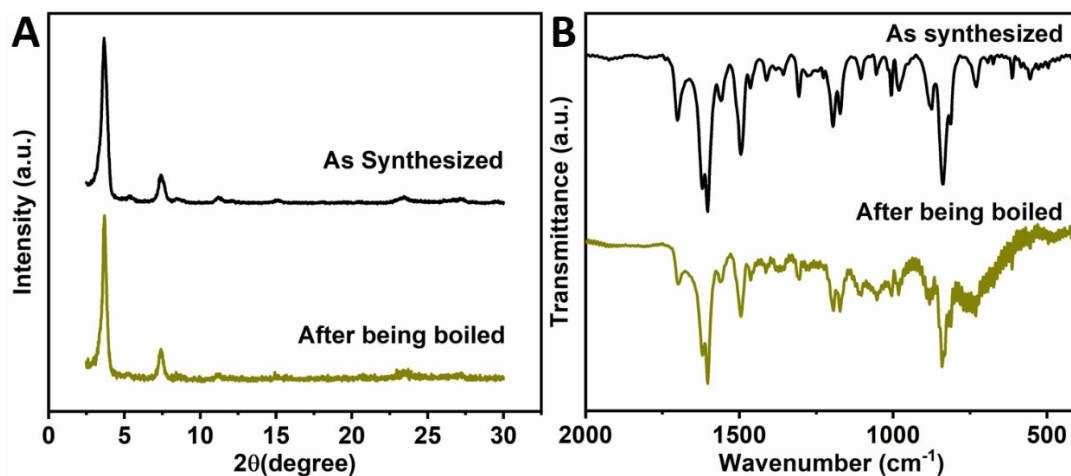


**Figure S21.** A) PXRD patterns and B) FTIR spectra of Pyurea-COF before and after being boiled in hot water (80 °C) for 8 hours.

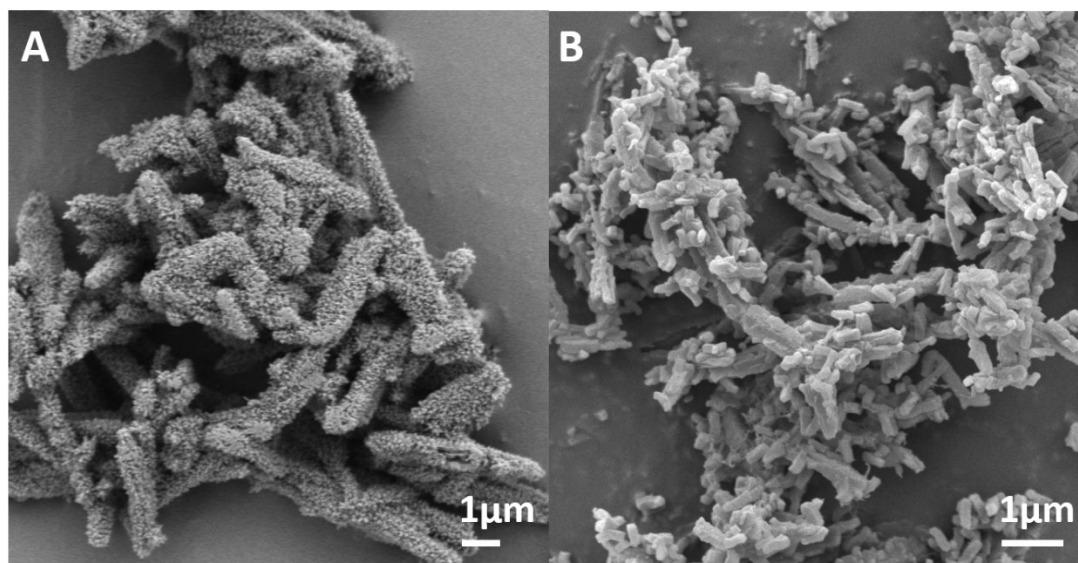


**Figure S22.** SEM images of A) Pythz-COF and B) Pyurea-COF after being boiled in hot water (80 °C) for 8 hours.

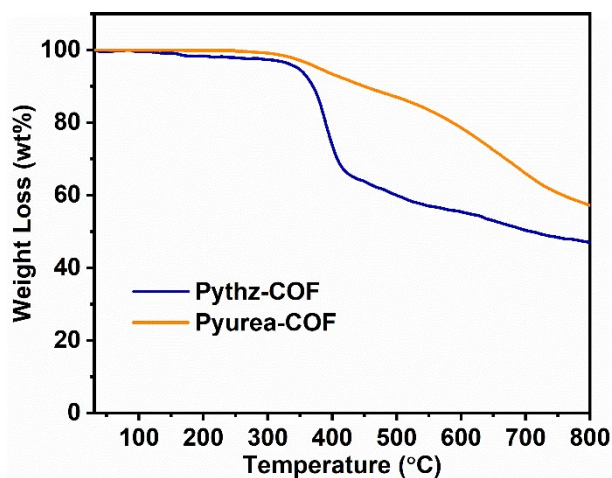


**Figure S23.** TGA profiles of Pythz-COF and Pyurea-COF after being boiled in hot water (80 °C) for 8 hours.

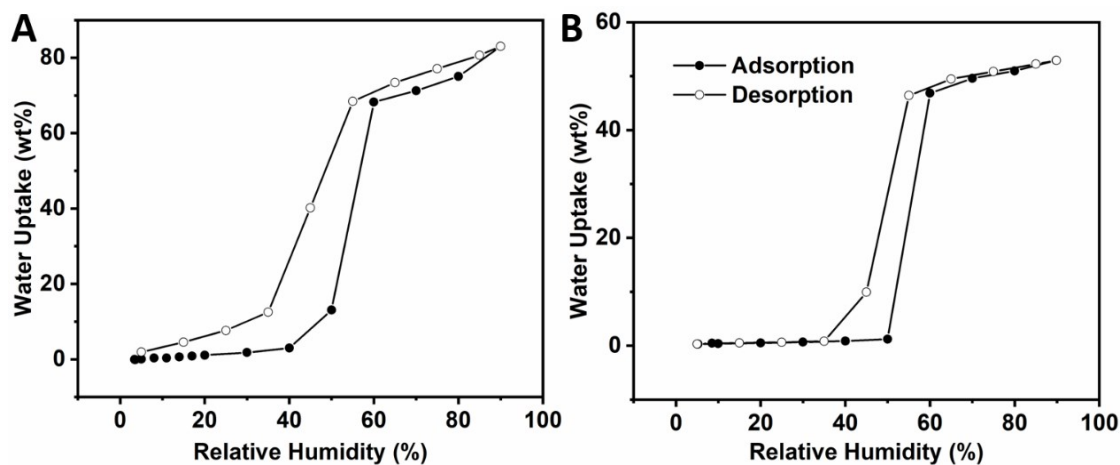


**Figure S24.** Water sorption analysis on A) Pythz-COF and B) Pyurea-COF after being boiled in hot water (80 °C) for 8 hours in the relative humidity range between 0% and 90% measured at 298K.

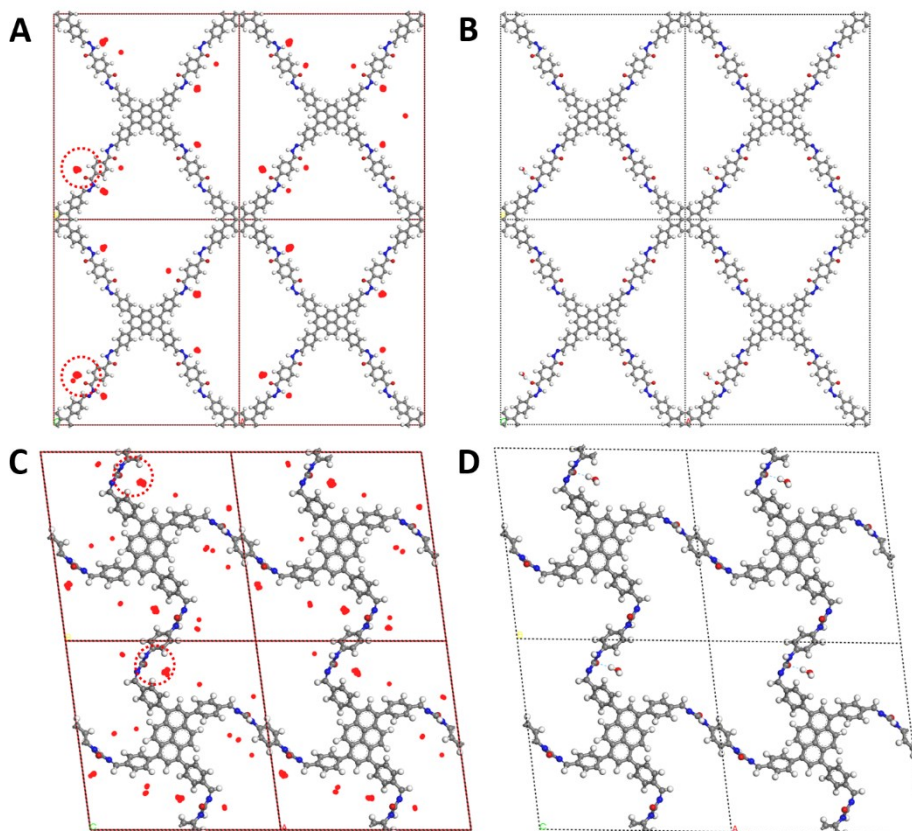


**Figure S25.** Simulated adsorption location of H<sub>2</sub>O in A) Pythz-COF and C) Pyurea-COF and H<sub>2</sub>O is most likely to occur in the red circle (The area of red dots is proportional to the probability of H<sub>2</sub>O occurrence); Theoretical calculation on hydrogen bonds between B) Pythz-COF and D) Pyurea-COF (grey: C, blue: N, white: H, red: O).

### 3. Reference

- 1) Y. Chen, C. Zhang, J. Xie, H. Li, W. Dai, Q. Deng and S. Wang, *Anal Chim Acta*, 2020, **1109**, 114-121.
- 2) H. L. Qian, C. Dai, C. X. Yang and X. P. Yan, *ACS Appl Mater Inter*, 2017, **9**, 24999-25005.
- 3) H. Q. Yin, F. Yin and X. B. Yin, *Chem Sci*, 2019, **10**, 11103-11109.
- 4) W. Ma, S. Jiang, W. Zhang, B. Xu and W. Tian, *Macromol Rapid Commun*, 2020, e2000003.
- 5) B. Li, W. Wang, Z. Hong, E. M. El-Sayed and D. Yuan, *Chem Commun*, 2019, **55**, 6926-6929.
- 6) A. Douvali, A. C. Tsipis, S. V. Eliseeva, S. Petoud, G. S. Papaefstathiou, C. D. Malliakas, I. Papadas, G. S. Armatas, I. Margiolaki, M. G. Kanatzidis, T. Lazarides and M. J. Manos, *Angew Chem Int Ed*, 2015, **54**, 1651-1656.
- 7) S. Pawar, U. K. Togiti, A. Bhattacharya and A. Nag, *ACS Omega*, 2019, **4**, 11301-11311.
- 8) J. Wang, J. Wang, W. Xiao, Z. Geng, D. Tan, L. Wei, J. Li, L. Xue, X. Wang and J. Zhu, *Anal Methods*, 2020, **12**, 3218-3224.
- 9) T. Wehner, M. T. Seuffert, J. R. Sorg, M. Schneider, K. Mandel, G. Sextl and K.



- Müller-Buschbaum, *J Mater Chem C*, 2017, **5**, 10133-10142.
- 10) H. L. Nguyen, N. Hanikel, S. J. Lyle, C. Zhu, D. M. Proserpio and O. M. Yaghi, *J Am Chem Soc*, 2020, **142**, 2218-2221.
- 11) L. Stegbauer, M. W. Hahn, A. Jentys, G. Savasci, C. Ochsenfeld, J. A. Lercher and B. V. Lotsch, *Chem Mater*, 2015, **27**, 7874-7881.
- 12) B. P. Biswal, S. Kandambeth, S. Chandra, D. B. Shinde, S. Bera, S. Karak, B. Garai, U. K. Kharul and R. Banerjee, *J Mater Chem A*, 2015, **3**, 23664-23669.
- 13) S. Karak, S. Kandambeth, B. P. Biswal, H. S. Sasmal, S. Kumar, P. Pachfule and R. Banerjee, *J Am Chem Soc*, 2017, **139**, 1856-1862.
- 14) D. Mullangi, S. Nandi, S. Shalini, S. Sreedhala, C. P. Vinod and R. Vaidhyanathan, *Sci Rep*, 2015, **5**, 10876.
- 15) Y. Byun and A. Coskun, *Angew Chem Int Ed Engl*, 2018, **57**, 3173-3177.
- 16) Mahmoud M. Abdelnaby, A. M. Alloush, N. A. A. Qasem, B. A. Al-Maythalony, R. B. Mansour, K. E. Cordova and O. C. S. Al Hamouz, *J Mater Chem A*, 2018, **6**, 6455-6462.
- 17) P. M. Schoenecker, C. G. Carson, H. Jasuja, C. J. J. Flemming and K. S. Walton, *Ind Eng Chem Res*, 2012, **51**, 6513-6519.
- 18) F. Jeremias, V. Lozan, S. K. Henninger and C. Janiak, *Dalton Trans*, 2013, **42**, 15967-15973.